ELSEVIER

Catalysis Today 50 (1999) 159–172

CATALYSIS TODAY

Computer-assisted mechanistic modeling of *n*-hexadecane hydroisomerization over various bifunctional catalysts

Tahmid I. Mizan, Michael T. Klein*

Department of Chemical Engineering, University of Delaware, Newark, DE 19716, USA

Abstract

Graph theoretic concepts were exploited to construct candidate computer models describing the hydroisomerization of *n*-hexadecane over bifunctional catalysts at a mechanistic level. The molecules and carbenium ions were represented as atomic connectivity matrices and the reactions as matrix operations. The computer-generated models were then automatically converted to a set of ordinary differential equations representing the reactions in a plug flow reactor. Typical diagnostics for the model building process indicate that models containing about 1000 species (molecules and ions) and 3000 reactions could be generated in around 1000 CPU seconds. Thus, some 25 candidate hydroisomerization models were built and evaluated through qualitative and quantitative comparisons with experimental data. The resulting best model was further pruned by removing extraneous reactions which did not result in observable products. This model was tuned against experimental data on three different catalysts at different temperatures. Good agreement between model predictions and experimental data was obtained. Trends in the fundamental mechanistic rate constants obtained from the model fitting process were in harmony with the trends in the acid and metal loadings of the catalysts. Thus, fundamental mechanistic modeling can provide valuable insight into the nature of the catalytic action.

Keywords: Bifunctional catalysts; Hydroisomerization; Hexadecane

1. Introduction

Hydroisomerization may be used as a process for the yield-preserving removal of long chain *n*-alkanes from lubricating oils in order that these have acceptable pour points and cold flow properties [1]. In essence, it holds promise as a dewaxing operation. The chemistry of hydroisomerization as a dewaxing process involves the conversion of normal paraffins to less waxy branched isoparaffins without creating species which fall outside the lube oil range.

The current major processes for removing wax from refined wax distillate (RWD), which is the precursor to lubricating oil base stocks, are catalytic and solvent dewaxing. A typical light refined wax distillate may have a modal *n*-alkane carbon number of 24 with minimum and maximum values of 16 and 36, respectively [2]. In catalytic dewaxing the *n*-alkanes are selectively cracked over a zeolite catalyst having a pore size which admits only normal paraffins and normal-paraffin-like side chains. In solvent dewaxing the wax removal is based on its solubility when dissolved in a suitable solvent. The proposed hydro-

*Present address: Rutgers University, College of Engineering, Office of the Dean, B204, 98 Brett Road, Piscataway, New Jersey 08854-8058; Tel.: +1-7324454453; fax: +1-7324457067; e-mail: mtklein@jove.rutgers.edu

0920-5861/99/$ – see front matter
PII: S0920-5861(98)00473-8

isomerization scheme would be superior to both conventional lubricant dewaxing processes because these reject part of the feed either as cracking products or as was removed and, therefore, have a reduced yield of dewaxed product. This reduction in yield is approximately proportional to the amount of *n*-alkanes present, which may be of the order 10–15%. Thus, hydroisomerization appears to be a logical choice as a dewaxing process by which normal paraffins may be converted to less waxy branched isoparaffins without creating species which fall outside the lube oil range. Unfortunately, this choice is not without its drawbacks, because hydroisomerization is invariably accompanied by some hydrocracking. To complicate the issue further, the more reactive isoparaffins present in the feed are often observed to crack long before significant isomerization of normal paraffins can begin [1]. The object, then, is to minimize the selectivity to the cracking pathways while achieving a satisfactory degree of isomerization.

While there have been a number of experimental investigations [1,3,4] of hydrocracking and hydroisomerization of paraffins up to hexadecane, many mechanistic aspects and catalyst effects are still a matter of debate. Taylor and Petty [1] have investigated hydroisomerization of Pd impregnated zeolites. They found that the SAPO-11 catalyst was capable of isomerizing the normal paraffins in the feed without resulting in large yield losses due to the cracking of isoparaffins. While the Taylor and Petty [1] study demonstrated the feasibility of a hydroisomerization-based dewaxing process, it does not provide any information about the molecular composition of the product. Therefore, this work is not useful for extracting kinetic information which can be used to develop fundamental molecule-based kinetic models. Girgis and Tsao [5] have published data for the hydroisomerization of *n*-hexadecane on various catalysts. These data have been used in the present work to calibrate and evaluate various computer-generated models.

A number of lumped parameter models of hydrocracking and hydroisomerization exist [4,6,7]. More recently a more fundamental model [8] for the hydroisomerization of *n*-octane on Pt/US Y-zeolite has been published. However, no comprehensive, molecule-based models exist that are able to handle feedstocks with heavy paraffinic components such as C_{16}–C_{36}, which would be more representative of the boiling range of dewaxing feedstocks [2]. Such a model would be useful in probing dewaxing process technologies. In this work, we examine hydroisomerization of *n*-hexadecane as a vehicle to establish a modeling protocol and kinetic parameters which can, in the future, be used to model a typical feed.

2. Computer-assisted model building

On a mechanistic level, hydroisomerization of long chain paraffins can involve a network of a very large number of species and reactions. Deriving such large molecular kinetic models by hand can be a tedious and time-consuming process. However, such models are usually built upon a few basic chemical principles tempered with the model builder's observations, experience, and intuition which can be summarized as a set of rules or heuristics. Such circumstances suggest that given a rigorous framework computers may be used to apply these chemical principles and rules and thereby build a kinetic model.

The framework for this model building process has been developed exploiting notions of graph theory. A molecule, which is set of atoms connected by bonds, may be conceptualized as a set of vertices connected by edges, or to be more precise, a graph. The graph of a molecule can be represented by a bond electron (connectivity) matrix [9]. For a typical reaction the connectivities of only a few of the atoms in the involved molecules change. This implies that a reaction can be represented by the change in the connectivity of only a few atoms. The connectivity matrices of the reactants can be combined into an augmented reactant matrix, which, after permutation, gives the reduced matrix for the reactants, containing the connectivities of only those atoms whose connectivity changes in the reaction process (that is, the reaction site). The bond breaking and forming for a reaction can be represented compactly in the form of a matrix operator formally called the reaction matrix [9]. The addition of this reaction matrix operator to the reduced matrix transforms the reactants to products. It is noteworthy that the reaction matrix for any particular type of reaction is the same irrespective of the participating reactants. Details of these concepts and methods may be found elsewhere [9–11].

The computer-assisted model building process consists of three conceptual stages. In the first stage, a reaction network is generated from the input reactant graphs using the reaction matrices and rules. This is achieved through the use of the *NetGen* [9] model building tools, together with the *NetGen:Hydroisomerization* driver. In the second stage, this reaction network is converted into a set of algebraic or differential equations expressed as C code, using the *OdeGen* parsing code [9]. In the final stage, these equations are solved and optimized against experimental data.

Various modifications were made to the existing family of *NetGen-OdeGen* codes [9] to obtain the model in the required format. The modifications are described below. The model builder was modified to classify the graphcodes of the molecules into the families of paraffins, isoparaffins, olefins, iso-olefins, and carbenium ions. It also identified the degree of branching and the type of carbenium ion. The reactions of each family member were separately handled by incorporating an additional filter on the type of reactions allowed for each compound class. Various filters were also used to allow reactions of only certain types of carbenium ions with a certain number of branches. These restrictions are discussed in detail later. The products obtained were checked for isomorphism (uniqueness) and then were identified for the compound type. The rate expressions were written in a file which served as the input to *OdeGen*. The mechanistic hydroisomerization model generated by *OdeGen* can be incorporated in a modular manner to reactor type as discussed below. The present version of *OdeGen* produces a C code for rate expressions which can be modularly linked to C code for a plug flow reactor (Pfr) with molar expansion, a batch reactor (Batch), a continuous stirred tank reactor with molar expansion (CstrE), a continuous stirred tank reactor (Dcstr). The rate constants can be expressed as linear free energy relationships (LFERs) if required. The reactor codes for Pfr, Batch, and Dcstr use the DASSL code [12] to integrate the ordinary differential equations. The CstrE code uses the Newton–Kantorovich method to solve the system of non-linear algebraic equations. The required Jacobian matrix was generated numerically and a robust matrix inversion code [13] which can handle the very large matrix inversion problems which arise for our systems is used to invert the Jacobian matrix.

3. Model building for hydroisomerization

Hydroisomerization on bifunctional catalysts proceeds by the sequential action of the metal and acid functions on the paraffinic feed. First, the paraffin is dehydrogenated by the metal hydrogenation/dehydrogenation function. The resulting olefin is protonated at the acid site, thus producing a alkylcarbenium ion. The carbenium ion undergoes a sequence of isomerization and cracking reactions on the acid sites. The resulting carbenium ions can deprotonate to form olefins. These reactions, together with the metal function-facilitated hydrogenation of any olefins that form, result in the observed product spectra. The carbenium ion reactions typically observed are protonated-cyclopropane-intermediate-mediated (PCP) branching, hydride shift, methyl shift, and beta scission. The higher the carbon number of the feed, the more effectively the cracked products are prevented from undergoing secondary branching reactions [14]. Thus, once a carbenium ion has cracked through beta scission, it is not expected to isomerize or crack further; rather, it will probably deprotonate and hydrogenate to form the corresponding paraffin. Since primary and methyl carbenium ions are relatively unstable, reactions which generate them may be neglected [8]. Hydrogenolysis only occurs with very high hydrogenation site to acid site ratio [3] and thus was neglected in the present modeling approach.

In this study, mechanistic kinetic models for the hydroisomerization on *n*-hexadecane were established. The *NetGen:Hydroisomerization* model builder has the capability execute a variety of reactions, all of which may be toggled on and off in a particular model. These reactions are:

1. dehydrogenation of alkane to alkene,
2. protonation of alkene to form carbenium ion,
3. protonated-cyclopropane-intermediate mediated branching,
4. hydride shift in carbenium ion,
5. methyl shift in carbenium ion,
6. cracking through beta scission,
7. deprotonation of carbenium ion, and
8. hydrogenation of alkene.

These reactions are schematically represented in Fig. 1. The first row in Fig. 1 shows the dehydrogenation of a paraffin at a metal site to form the

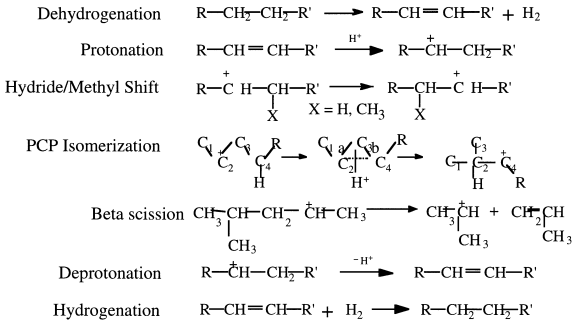

Fig. 1. Reaction families for hydroisomerization.

corresponding olefin, which then undergoes protonation at an acid site to form a carbenium ion as shown in the second row. These carbenium ions can undergo 1, 2 hydride or methyl shift reactions where a charge adjacent to a hydride or methyl group is interchanged with either of the latter. Carbenium ions can undergo protonated-cyclopropane-intermediate-mediated branching as shown in row 4 of Fig. 1. Here carbon atoms numbered 2, 3, and 4 form a cyclopropane structure and the proton is attached either at carbon 4 or along the 2–4 edge. Once this intermediate is formed, it can lead to two different branched structures through breaking of either the 2–3 bond (labeled a) or the 3–4 bond (labeled b). In Fig. 1 only the b type isomerization is shown. Carbenium ions can also undergo beta scission (row 5) where the bond beta to the position of the charge breaks to form a smaller carbenium ion and an olefin with the double bond at the position of the original charge. All carbenium ions can deprotonate and the resulting olefins can saturate to form the corresponding paraffins. The reaction matrices and reactions sites corresponding to these reaction families are shown in Table 1. A mechanistic kinetic model for the hydroisomerization of *n*-hexadecane would consist of various C_{16} paraffin isomers,

Table 1
Reaction sites and matrices for elementary steps in hydroisomerization

Name	Reaction site	Reaction matrix
Dehydrogenation	CH_2–CH_2	$\begin{bmatrix} 0 & 1 & -1 & 0 \\ & 1 & 0 & 0 & -1 \\ & -1 & 0 & 0 & 1 \\ & 0 & -1 & 1 & 0 \end{bmatrix}$
Protonation	C=C	$\begin{bmatrix} 0 & -1 & 1 \\ & -1 & 0 & 0 \\ & 1 & 0 & 0 \end{bmatrix}$
PCP-isomerization	C+–C–C–H	$\begin{bmatrix} 0 & 0 & 1 & 0 \\ & 0 & 0 & -1 & 1 \\ & 1 & -1 & 0 & -1 \\ & 0 & 1 & -1 & 0 \end{bmatrix}$
H/Me shift	H–C–C+/C–C–C+	$\begin{bmatrix} 0 & 0 & 1 \\ & 0 & 0 & -1 \\ & 1 & -1 & 0 \end{bmatrix}$
Beta-scission	C+–C–C	$\begin{bmatrix} 0 & 1 & 0 \\ & 1 & 0 & -1 \\ & 0 & -1 & 0 \end{bmatrix}$
Deprotonation	H–C–C+	$\begin{bmatrix} 0 & 1 & -1 \\ & 1 & 0 & 0 \\ & -1 & 0 & 0 \end{bmatrix}$
Hydrogenation	C=C	$\begin{bmatrix} 0 & -1 & 1 & 0 \\ & -1 & 0 & 0 & 1 \\ & 1 & 0 & 0 & - \\ & 0 & 1 & -1 & 0 \end{bmatrix}$

C_{16} olefins, C_{16} carbenium ions and various lower carbon number cracking products (paraffins) and their precursors (olefins and carbenium ions). At a carbon number of 16 about 50 000 paraffinic isomers and about 500 000 olefinic isomers are possible (including stereoisomers) [15]. It is obvious that a reaction network which includes every possible paraffin, olefin and carbenium ion will have an inordinately large number of species. Thus, in order to produce a mechanistic model which is of a size reasonable enough to facilitate rapid solution on available computational resources, certain reaction rules must be invoked. These rules are based on knowledge of thermochemistry, prior knowledge of which types of reactions or species might be kinetically insignificant, statistical arguments, and empirical experimental knowledge about the product spectrum or reactions. The following rules assisted the model building process for the hydroisomerization of *n*-hexadecane:

1. All carbenium ions less than C_{16} will deprotonate and hydrogenate. This rule is based on the observations of Coonradt and Garwood [14] discussed earlier.
2. No primary carbenium ions are allowed to form. This rule is based on the observations of Baltanas et al. [8].
3. The tertiary carbenium ion is stable and unlikely to undergo PCP-isomerization.
4. PCP-isomerization either increases the number of branches or the length of the side chains.
5. PCP-isomerization was not allowed to form geminal branches. This is because quarternary carbons are rarely observed experimentally.
6. PCP-isomerization was not permitted to form vicinal branches. Branches alpha to existing branches are also rarely observed experimentally.
7. The maximum side chain length is 2.
8. A maximum of three branches was allowed.
9. Dehydrogenation was permitted everywhere for straight chain paraffins and only beta to branches of isoparaffins for some of the models developed.
10. Secondary cracking (beta scission) was not allowed. This relates to the observations of Coonradt and Garwood [14].
11. C-type beta scission, in which a secondary carbenium ion forms another secondary carbenium ion, was not allowed for some of the models developed. C-type beta scission is sometimes considered to be negligible [3].
12. No hydride transfer (H-abstraction) was allowed.
13. The number of allowable PCP-isomerizations, methyl shifts, and hydride shifts was made to be a function of number of branches in the reactant carbenium ion. This allowed the product spectrum to be tailored to a desired combination while keeping the size of the model sufficiently small as to be solvable.

The first phase of the modeling operation consisted of building various models subject to various combinations of rules 9, 11 and 13 mentioned above. All other rules were held constant. Varying the allowable number of PCP-isomerization reactions, methyl shifts, and hydride shifts provided control of the size of the models in terms of both the number of species and reactions involved. If an unlimited number of PCP-isomerizations were allowed, the number of isomeric species would rapidly build up to an intractable number which would exceed the physical capacity of the available computer memory (or indeed, analytical chemistry resolution). The objective, then, was to get as small a model as possible and yet retain the desired product spectrum. In particular, the mono-branched C_{16} species, which are analytically discernible, should all be present in the product spectrum. Experimentally, mostly methyl and ethyl mono-branched species are observed. There are seven methyl and five ethyl mono-branched C_{16} paraffins and any viable model should be able to produce these in its product spectrum. The di- and multi-branched C_{16} paraffins are harder to distinguish analytically and are usually lumped together. Therefore, a representative sample of these is sufficient to model this lump. In addition, the model should be able to predict a variety of cracked paraffins.

Twenty-five different models with various limitations on PCP-isomerizations, methyl shifts, hydride shifts were built and examined with respect to size and product spectrum. The results are presented in Table 2. The allowable limits on the number of different reactions were made a function of the degree of branching of the reactant carbenium ion. Each model produced a different product spectrum or had different characteristics with respect to the number of species or number of reactions. The models were built to differ-

Table 2
Effect of constraining number of allowed reactions on hydroisomerization models

Model	Allowed reaction constraints									Rank[c]	Products				Model characteristics					
	PCP-isomerization			Methyl shift			Hydride shift				C_{16}-paraffins			Cracked paraffins	Species	Ions	Olefins	Reactions	Build time (s)	Memory (KB)
	0-br	1-br	2-br	1-br	2-br	3-br	1-br	2-br	3-br		1-br	2-br	3-br							
5.0	∞	∞	∞	∞	∞	∞	∞	∞	∞	5	12	5	0	0	487	277	191	1335	222	41 588
5.1[a]	8	8	8	8	8	8	8	8	8	5	7	2	0	0	178	63	104	444	85	11 668
5.2	8	8	8	8	8	8	8	8	8	5	7	2	0	0	142	63	68	372	70	12 484
5.3	8	8	8	0	0	0	8	8	8	5	7	2	0	0	125	54	60	329	63	12 196
5.4	8	8	8	0	0	0	0	0	0	5	7	2	0	0	103	43	49	276	58	11 468
5.5	16	16	16	16	16	16	16	16	16	5	10	3	0	0	217	100	102	585	109	19 604
5.9	32	32	16	0	0	0	8	8	8	5	12	5	0	0	244	103	122	677	122	23 744
5.12	20	20	20	0	0	0	0	0	0	5	12	4	0	0	186	80	88	526	98	20 496
5.13[b]	20	20	20	0	0	0	0	0	0	5	12	4	0	0	208	91	99	537	104	20 572
10.0	∞	∞	∞	∞	∞	∞	∞	∞	∞	10	Insufficient memory									
10.1[a]	8	8	8	8	8	8	8	8	8	10	8	9	4	17	788	334	414	2329	417	41 160
10.2	8	8	8	8	8	8	8	8	8	10	8	9	4	17	520	215	265	1455	242	46 340
10.3	8	8	8	0	0	0	8	8	8	10	7	4	3	18	382	156	192	1049	177	32 676
10.4	8	8	8	0	0	0	0	0	0	10	7	4	3	10	320	139	155	884	150	2 8704
10.5	16	16	16	16	16	16	16	16	16	10	11	16	11	30	950	396	484	2666	448	80 148
10.9	32	32	16	0	0	0	8	8	8	10	12	17	1	30	891	387	442	2537	398	73 228
10.12	20	20	20	0	0	0	0	0	0	10	12	12	6	22	722	314	354	2014	327	60 872
10.13[b]	20	20	20	0	0	0	0	0	0	10	12	12	6	29	799	345	393	2207	345	62 288
10.14[b]	16	32	32	0	0	0	0	0	0	10	11	16	9	35	978	424	481	2693	428	74 404
10.15[b]	20	20	32	0	0	0	0	0	0	10	12	12	9	31	839	364	409	2321	361	65 208
10.16[b]	20	32	32	0	0	0	0	0	0	10	12	16	9	35	991	430	487	2736	419	76 168
10.17[b]	16	16	16	16	16	16	16	16	16	10	11	16	11	41	1073	448	544	3004	471	83 812
10.18[b]	20	16	16	8	8	8	8	8	8	10	11	13	7	33	898	370	462	2516	398	71 408
15.2	8	8	8	8	8	8	8	8	8	15	8	9	4	21	713	306	363	2062	307	54 560
15.13[b]	20	20	20	0	0	0	0	0	0	15	12	12	6	61	1403	586	724	3962	561	94 588

[a]Allow all dehydrogenations.
[b]Allow C-type beta scission.
[c]Maximum product rank includes carbenium ions.

ent ranks or product generations from 5 to 15. It is clear from Table 2 that the rank 5 models were not sufficient to produce the cracked products. This is because some amount of branching must be present before cracking can begin since primary carbenium ions were not allowed. Not restraining the number of PCP-isomerizations can lead to a divergence in the model building process, as shown for model 10.0. Again, too few PCP-isomerizations will mean an incomplete product spectrum: model 10.2 allows only eight PCP-isomerizations for 0-branch carbenium ions and forms only eight of the 12 mono-branched C_{16} paraffins, whereas model 10.9, which allows 32 PCP-isomerizations for 0-branch carbenium ions, forms all 12 paraffins.

Three other observations may be made by scrutinizing Table 2. First, methyl and hydride shifts do not have a profound role in shaping the experimentally discernible C_{16} paraffin product spectrum, but do increase the size of the model. This is not to say that these reactions are not important. Indeed, they may be important in achieving the right kinetic balance when solving the model particularly when detailed, molecule-specific product composition is available. Second, all dehydrogenations of branched species also do not affect the observable product spectrum. They also greatly increase the size of the model by increasing the number of olefins produced. By imposing some sort of rule on dehydrogenations (rule 9), the size of the model may be reduced without compromising the product spectrum. Last, allowing C-type beta scission, in which a secondary carbenium ion cracks to form another secondary carbenium ion (rule 11) and an olefin was found to have a profound effect on the ability of the model to fit experimental data. This aspect of rule 11 is discussed in the next section. Turning off rule 11 (that is, allowing C-type beta scission) merely increases the number of cracked paraffinic products observed.

4. Results and discussion

The models were optimized using published experimental data [5] for the hydroisomerization of *n*-hexadecane on Pt/Si–Al (silica–alumina) catalyst at 553 K. The final or optimal form of the hydroisomerization model (10.13) contained 799 components and 2207 reactions. This model was molecularly explicit and included 344 carbenium ions. The C_{16} isomers in this model are tabulated in Table 3. These include all the possible mono-methyl and mono-methyl isomers and a representative selection of multi-branched isomers. Table 4 gives the identities of the cracking products. The ordinary differential equations representing the reaction model written specifically for a plug flow reactor were solved using DASSL [12]. In solving the model only eight rate constants were used for dehydrogenation, protonation, deprotonation, PCP-isomerization to multi-branched ions, reverse PCP-isomerization for multi-branched ions, and beta scission, respectively. The hydrogenation rate constant was determined from the dehydrogenation–hydrogenation equilibrium constant [16]. Even with such a small set of parameters, a fairly good fit of the experimental data was possible, as is evident in Fig. 2. The predicted conversions, molar yields of cracking products, and molar yields of mono-branched C_{16} paraffins were excellent. The molar yields of multi-branched paraffins were, however, underpredicted. The model tuning was performed using the optimization code GREGG [17]. Model 10.13 took an inordinately long time (several weeks) to optimize because a ''once through'' solution of the set of ordinary differential equations required about 8000 s on an IBM

Table 3
C_{16} paraffinic products

Mono-branched C_{16} paraffins	Multi-branched C_{16} paraffins
3-Methyl-pentadecane	2-4-Dimethyl-tetradecane
2-Methyl-pentadecane	3-5-Dimethyl-tetradecane
4-Methyl-pentadecane	4-6-Dimethyl-tetradecane
5-Methyl-pentadecane	5-7-Dimethyl-tetradecane
6-Methyl-pentadecane	2-Methyl-4-ethyl-tridecane
7-Methyl-pentadecane	3-Methyl-5-ethyl-tridecane
8-Methyl-pentadecane	4-Methyl-6-ethyl-tridecane
3-Ethyl-tetradecane	3-Ethyl-5-ethyl-tridecane
4-Ethyl-tetradecane	5-Methyl-7-ethyl-tridecane
5-Ethyl-tetradecane	4-Ethyl-6-methyl-tridecane
6-Ethyl-tetradecane	2-4-6-Trimethyl-tridecane
7-Ethyl-tetradecane	2-4-8-Trimethyl-tridecane
	2-4-7-Trimethyl-tridecane
	3-5-7-Trimethyl-tridecane
	3-5-9-Trimethyl-tridecane
	3-5-8-Trimethyl-tridecane
	3-5-Diethyl-dodecane
	4-6-Diethyl-dodecane

Table 4
Cracked paraffinic products

Carbon number	Paraffins
C_{13}	*n*-Tridecane
	2-Methyl-dodecane
	3-Methyl-dodecane
	4-Methyl-dodecane
C_{12}	*n*-Dodecane
	2-Methyl-undecane
	3-Methyl-undecane
	4-Methyl-undecane
C_{11}	*n*-Undecane
	2-Methyl-decane
	3-Methyl-decane
C_{10}	*n*-Decane
	2-Methyl-nonane
	3-Methyl-nonane
C_9	*n*-Nonane
	4-Methyl-octane
C_8	*n*-Octane
	4-Methyl-heptane
C_7	*n*-Heptane
	2-methyl-hexane
	3-Methyl-hexane
C_6	*n*-Hexane
	2-Methyl-pentane
	3-Methyl-pentane
C_5	*n*-Pentane
	2-Methyl-butane
C_4	*n*-Butane
	2-Methyl-propane
C_3	Propane

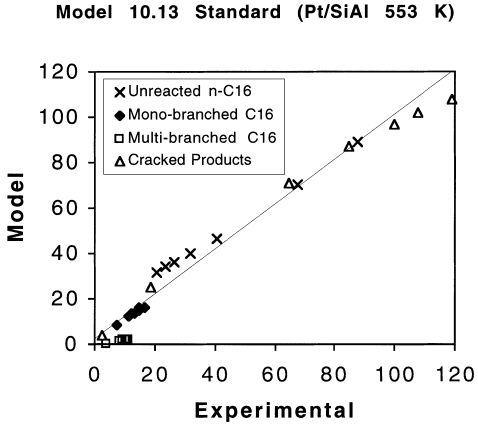

Fig. 2. Parity plot of molar yields for standard model 10.13 for Pt/SiAl at 553 K.

RS6000 computer. In order to reduce the solution time, the ''rank-based reaction restriction'' (RRR) rules were applied to the model building process. These rules are described below.

4.1. Rules for rank-based reaction restriction

Rank, for the purposes of this discussion, refers to the order of appearance of a product starting from the initial reactants which are considered to be of rank 0. Rank is used in the current model building process as a termination criterion. Thus, the model building process may be terminated at say rank 10 if all the known products have appeared by that rank. Since paraffins are the only observable products in the hydroisomerization of a paraffin, any branches of the reaction network which lead to terminal rank products which are not paraffins (that is, are either olefins or ions) are redundant and an unnecessary computational overhead. The ''rank-based reaction restriction'' rules essentially prevent reactions which will result in these unnecessary terminal rank products. These rules are summarized below. Disallow reactions based on the reactant rank:

no dehydrogenation if rank$\geq$MaxRank -3,
no protonations if rank$\geq$MaxRank -2,
no PCP-isomerizations if rank$\geq$MaxRank -1,
no methyl shifts if rank$\geq$MaxRank -1,
no hydride shifts if rank$\geq$MaxRank -1,
No beta scissions if rank$\geq$MaxRank, and
no deprotonations if rank$\geq$MaxRank,

where MaxRank is the maximum allowable (or termination) rank.

These rules were applied to model 10.13 to generate the RRR version, that is 10.13RRR. The savings in model solution time obtained using the RRR model over the standard model are quite startling. These models are compared in Table 5. The RRR version of the model has 40% fewer species and reactions but takes 2500% less time to solve. It should be noted that the standard and RRR models had identical observable (paraffinic) product spectra (as given in Tables 3 and 4).

Using the RRR version of model 10.13 afforded the rapid optimization using the data of Girgis and Tsao [5]. Fig. 3(a) shows the parity plot of the experimental

Table 5
Comparison of rank-based reaction restricted model with standard model

Model	Species	Ions	Olefins	Reactions	Build time (s)	Memory (KB)	Solve time (s)
Standard	799	345	393	2207	345	62 288	7825
RRR	496	172	263	1443	353	43 996	306

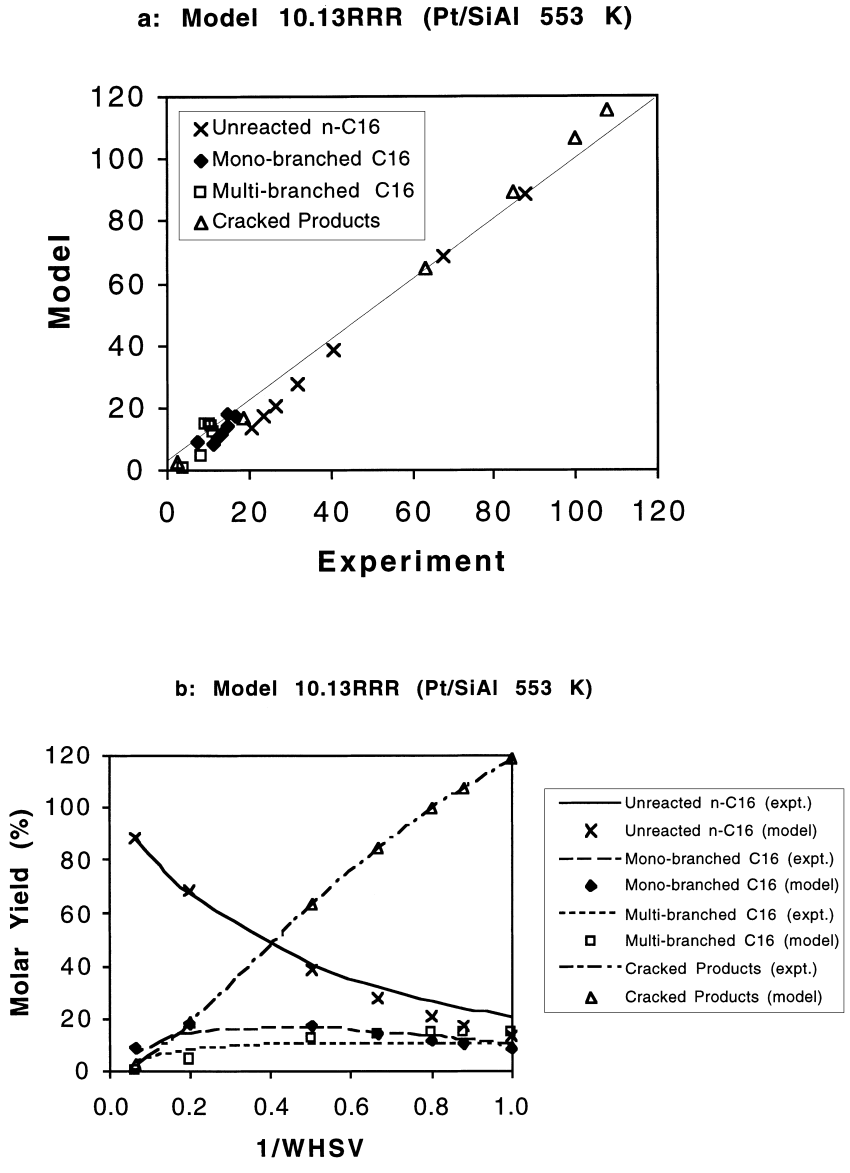

Fig. 3. Model 10.13RRR for Pt/SiAl at 553 K: (a) parity plot of molar yields, and (b) molar yield profiles.

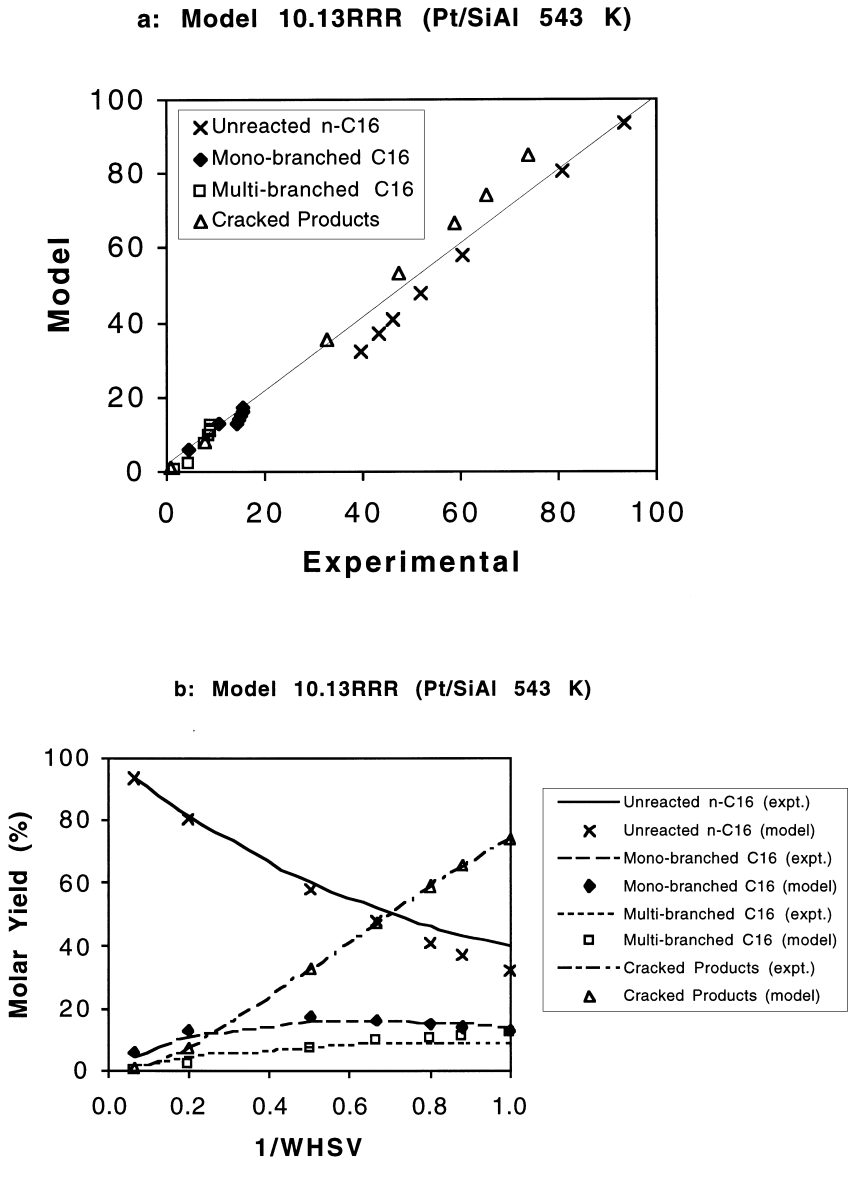

Fig. 4. Model 10.13RRR for Pt/SiAl at 543 K: (a) parity plot of molar yields, and (b) molar yield profiles.

data with the Pt/SiAl catalyst at 553 K versus that predicted by the model. The corresponding molar yield profiles across various residence times is depicted in Fig. 3(b). The agreement is very good although, the model does underpredict conversion slightly at lower space velocities. Fig. 4(a) and (b) show the fits of the model predictions against experiment for the same catalyst but at 543 K. The same model was used to fit the experimental data reported by Girgis and Tsao [5] for a Pt/MCM41 catalyst at 563 K. As depicted in Fig. 5(a) and (b), the fits were even better than for the amorphous catalyst. Finally, model 10.13RRR was fitted to experimental data for the Pt/Z (zeolite) catalyst at 573 K. Again, as Fig. 6(a) and (b) show the model reproduced the observed experimental trends perfectly.

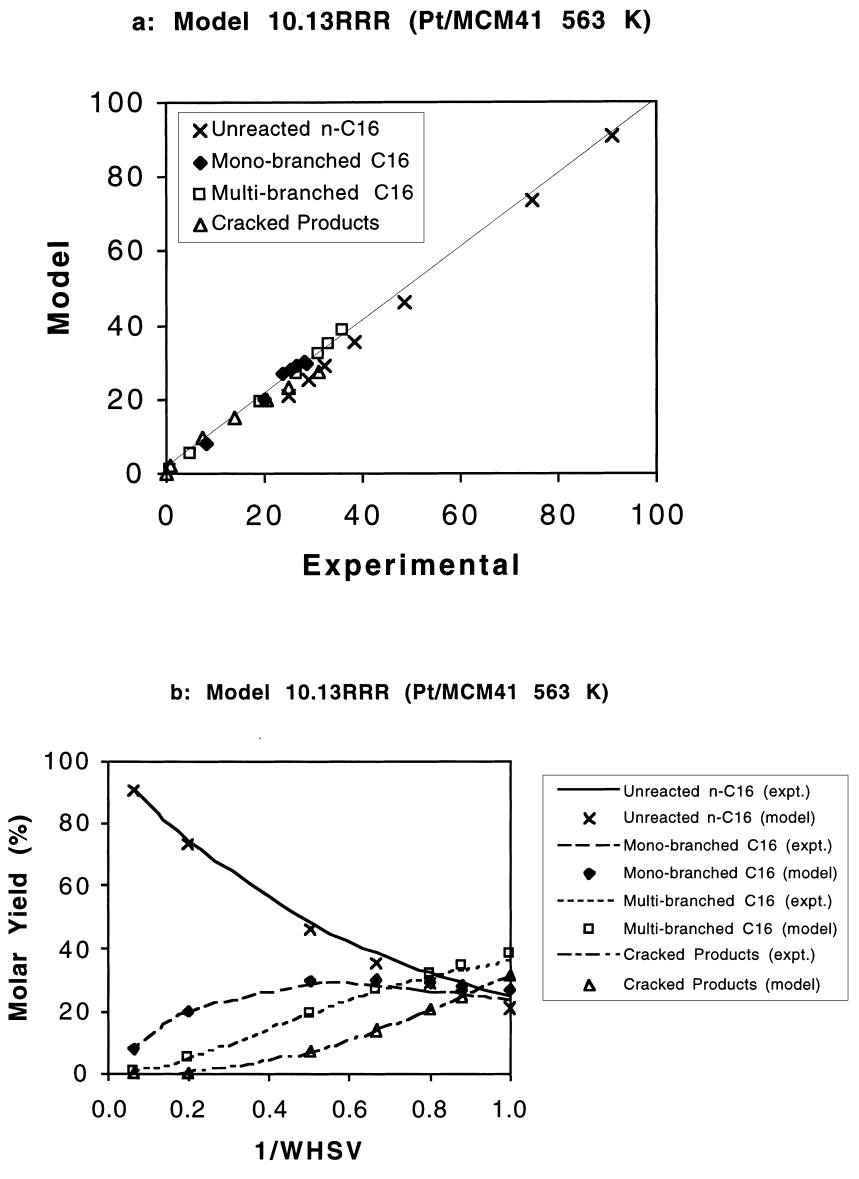

Fig. 5. Model 10.13RRR for Pt/MCM41 at 563 K: (a) parity plot of molar yields, and (b) molar yield profiles.

4.2. *Significant findings*

It is noteworthy that this approach was successfully applied to experimental results obtained from three different catalysts. Since these mechanistic models are fundamental in nature, that is, they represent the actual elementary reaction steps, it is reasonable to expect that the rate parameters obtained by fitting these models to experimental data should reveal fundamental information about the relative natures of the catalysts. The experimental data for the three catalysts were at different temperatures. Moreover, since either only one or two temperatures separated by 10 K were reported, the optimizations only produced point rate constants and not separate values for activation energies and pre-exponential factors. Nonetheless these point rate constants (Table 6) at 553 K for the Pt/SiAl catalyst, at 563 K for the Pt/MCM41 catalyst, and at

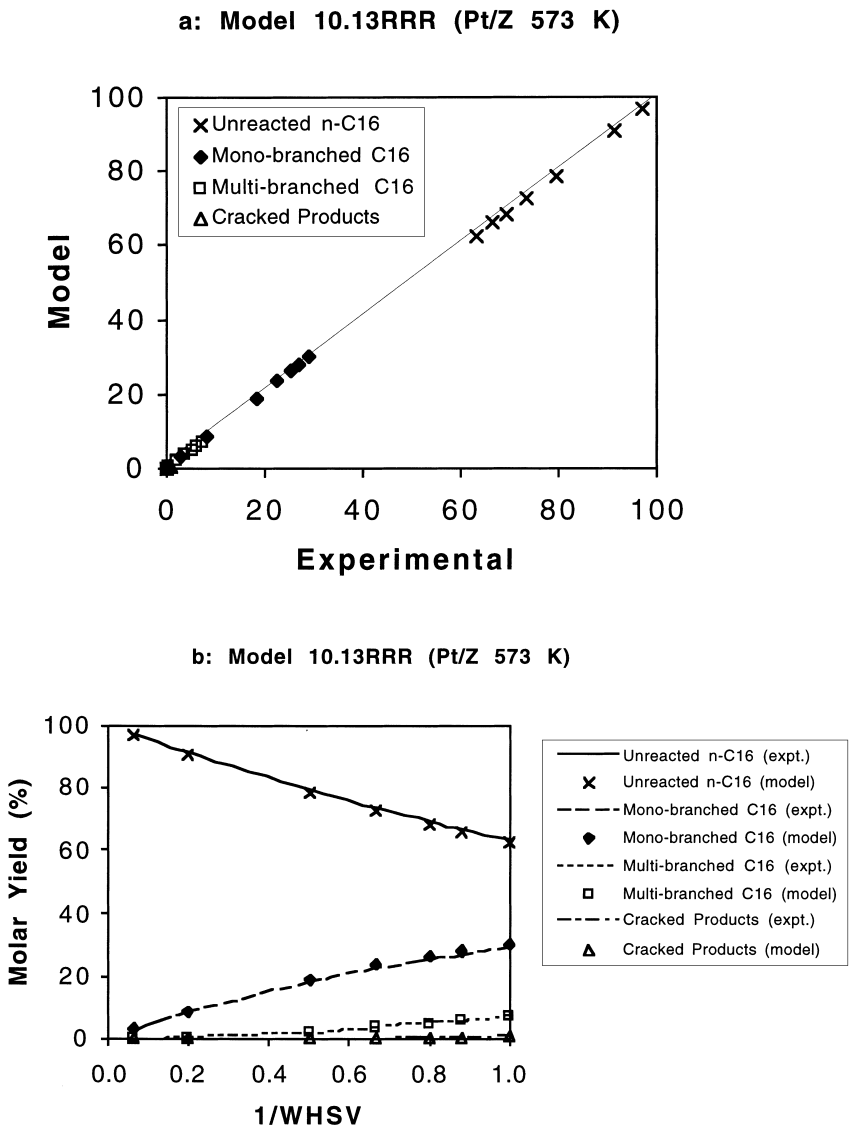

Fig. 6. Model 10.13RRR for Pt/Z at 573 K: (a) parity plot of molar yields, and (b) molar yield profiles.

573 K for the Pt/Z catalyst exhibited trends which agree with the known trends in the compositions of the catalysts. It may be mentioned that even if the rate constants are corrected to the same temperature (by assuming a reasonable set of common pre-exponential factors, the same trends are obtained). For instance, Fig. 7(a) shows that the log of the dehydrogenation rate constants for the three catalysts follows the order: Pt/MCM41>Pt/SiAl>Pt/Z and this is identical to the order of the platinum loading of the catalysts ([5], Table 2). The values for the log of the protonation rate constant shown in Fig. 7(a) are really product of the rate constant and the concentration of acid sites per gram of catalyst. The observed rate trend for this quantity as well as for the deprotonation rate constant is Pt/SiAl>Pt/MCM41, Pt/Z. This trend follows the total aluminium content of the three catalysts which is 8.6% for Pt/SiAl and 1% and 0.16% for Pt/MCM41 and Pt/Z, respectively. Fig. 7(b) shows the relative values of the other five rate constants. The beta

Table 6
Rate constants for various elementary steps on the three catalysts

	Pt/MCM41	Pt/SiAl	Pt/Z
k(Dehydrogenation)	1.4E+06	1.4E+03	1.4E+02
k(Protonation)×[H^+]	7.5E+03	4.0E+06	7.5E+03
k(PCP-mono)	3.9E+06	2.2E+05	2.2E+06
k(rPCP-mono)	1.1E+05	6.7E+02	6.6E+02
k(PCP-multi)	7.3E+07	5.2E+06	2.3E+07
k(rPCP-multi)	3.2E+01	1.0E-01	7.3E+00
k(Deprotonation)	6.2E+08	9.8E+09	1.8E+09
k(Beta scission)	2.0E+07	8.1E+06	1.3E+06

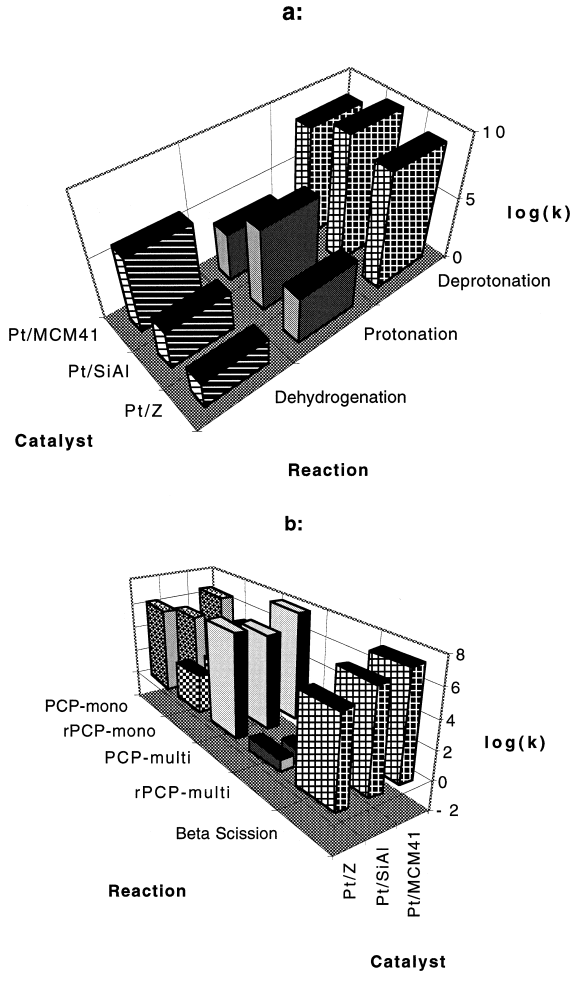

Fig. 7. Relative rates constants on various catalysts: (a) for forming olefins and carbenium ions, and (b) for isomerization and cracking.

scission rate constants for Pt/Z are lowest and reflect its low selectivity to cracking. The high cracking activity of the amorphous catalyst appears to be reflected in the greater net rate (lower reverse isomerization rate constant) of the PCP-isomerization to multi-branched species which then undergoes beta scission, rather than in the beta scission rate constant itself. Thus, it is clear that fundamental mechanistic kinetic models such as the ones reported in this study can provide valuable insight into the nature of the catalytic action.

5. Conclusions

This work demonstrates the use of automated kinetic model building for developing fundamental mechanistic models for heterogeneous catalytic reactions of a fairly high carbon number hydrocarbon species. It is shown that by judicious selection of reaction rules based on knowledge of thermochemistry, kinetics, empirical observations, and level of analytical resolution possible in experimental data, reasonably sized reaction models can be constructed. Moreover, these mechanistic models can represent experimental trends very well. This approach was demonstrated on three different catalyst systems and a comparison of the fitted rate constants for these three catalysts yielded fundamental insight into the nature of the catalytic action.

References

[1] R.J. Taylor, R.H. Petty, Appl. Catal. 119 (1994) 121.
[2] R.J. Taylor, A.J. McCormack, I. & E. C. Res. 31 (1992) 1731.
[3] F. Alvarez, F.R. Ribeiro, G. Perot, C. Thomazeau, M. Guisnet, J. Catal. 162 (1996) 179.
[4] J. Weitkamp, I. & E. C. Prod. Res. Dev. 21 (1982) 550.

[5] M.J. Girgis, Y.P. Tsao, I. & E. C. Res. 35 (1996) 386.
[6] M. Steijn, G.F. Froment, I. & E. C. Prod. Res. Dev. 20 (1981) 660.
[7] M.A. Baltanas, H. Vansina, G.F. Froment, I. & E. C. Prod. Res. Dev. 22 (1983) 531.
[8] M.A. Baltanas, K.K. Van Raemdonck, G.F. Froment, S.R. Mohedas, I. & E. C. Res. 28 (1989) 899.
[9] L.J. Broadbelt, S.M. Stark, M.T. Klein, I. & E. C. Res. 33 (1994) 790.
[10] L.J. Broadbelt, S.M. Stark, M.T. Klein, Chem. Eng. Sci. 49 (1994) 4991.
[11] L.J. Broadbelt, S.M. Stark, M.T. Klein, Computers Chem. Eng. 20 (1996) 113–129.
[12] K.E. Brenan, S.L. Campbell, L.R. Petzold, Numerical Solution of Initial-Value Problems in Differential-Algebraic Equations, Elsevier, New York, 1989, p. 115.
[13] H.T. Lau, A Numerical Library in C for Scientists and Engineers, CRC Press, Boca Raton, 1995, p. 634.
[14] H.L. Coonradt, W.E. Garwood, I. & E. C. Proc. Des. Dev. 3 (1964) 38.
[15] R.A. Alberty, C.A. Gehrig, J. Phys. Chem. Ref. Data 13 (1984) 1173.
[16] R.A. Alberty, C.A. Gehrig, J. Phys. Chem. Ref. Data 14 (1985) 803.
[17] W.E. Stewart, M. Carcotsios, J.P. Sorensen, AIChE J. 38 (1992) 641.